RESEARCH ARTICLE

THE PROTEIN SOCIETY WILEY

Crowding beyond excluded volume: A tale of two dimers

Gil I. Olgenblum[1] | Claire J. Stewart[2] | Thomas W. Redvanly[2] |
Owen M. Young[2] | Francis Lauzier[2] | Sophia Hazlett[2] | Shikun Wang[2] |
David A. Rockcliffe[3] | Stuart Parnham[4] | Gary J. Pielak[2,4,5,6] | Daniel Harries[1]

[1]Institute of Chemistry, the Fritz Haber Research Center, and the Harvey M. Kruger Center for Nanoscience & Nanotechnology, The Hebrew University, Jerusalem, Israel

[2]Department of Chemistry, University of North Carolina at Chapel Hill, Chapel Hill, North Carolina, USA

[3]Division of Molecular and Cellular Biosciences, National Science Foundation, Alexandria, Virginia, USA

[4]Department of Biochemistry & Biophysics, University of North Carolina at Chapel Hill, Chapel Hill, North Carolina, USA

[5]Lineberger Cancer Center, University of North Carolina at Chapel Hill, North Carolina, USA

[6]Integrative Program for Biological and Genome Sciences, University of North Carolina at Chapel Hill, Chapel Hill, North Carolina, USA

Correspondence
Gary J. Pielak, Department of Chemistry, University of North Carolina at Chapel Hill, Chapel Hill, NC, USA.
Email: gary_pielak@unc.edu

Daniel Harries, Institute of Chemistry, the Fritz Haber Research Center, and the Harvey M. Kruger Center for Nanoscience & Nanotechnology, The Hebrew University, Jerusalem 9190401, Israel.
Email: daniel.harries@mail.huji.ac.il

Review Editor: Aitziber L. Cortajarena

Abstract

Protein–protein interactions are modulated by their environment. High macromolecular solute concentrations crowd proteins and shift equilibria between protein monomers and their assemblies. We aim to understand the mechanism of crowding by elucidating the molecular-level interactions that determine dimer stability. Using ^{19}F-NMR spectroscopy, we studied the effects of various polyethylene glycols (PEGs) on the equilibrium thermodynamics of two protein complexes: a side-by-side and a domain-swap dimer. Analysis using our mean-field crowding model shows that, contrary to classic crowding theories, PEGs destabilize both dimers through enthalpic interactions between PEG and the monomers. The enthalpic destabilization becomes more dominant with increasing PEG concentration because the reduction in PEG mesh size with concentration diminishes the stabilizing effect of excluded volume interactions. Additionally, the partially folded domain-swap monomers fold in the presence of PEG, contributing to dimer stabilization at low PEG concentrations. Our results reveal that polymers crowd protein complexes through multiple conjoined mechanisms, impacting both their stability and oligomeric state.

KEYWORDS
dimerization, equilibrium thermodynamics, fluorine NMR, macromolecular crowding, polyethylene glycol

Gil I. Olgenblum, Claire J. Stewart, Thomas W. Redvanly, and Owen M. Young contributed equally to this study.

1 | INTRODUCTION

Cells sequester proteins at concentrations that can exceed 300 g/L (Theillet et al., 2014). However, biophysical studies are rarely performed at these concentrations despite abundant evidence (Speer et al., 2022) that folding intermediates observed in buffer may not be observed in cells, mutations with little effect in buffer alter cellular metabolism, and disordered proteins exhibit different ensembles in cells than they do in dilute solution. Understanding how crowding by cosolutes affects the equilibrium thermodynamics of protein–protein interactions is important because protein complexes are essential for signal transduction and cellular homeostasis (Theillet et al., 2014). Previously, we have systematically considered how crowding by polyethylene glycols (PEGs) and its monomer, ethylene glycol, impacts protein stability (Stewart et al., 2023). Here, we turn to protein–protein interactions.

We chose two reversibly formed homodimers, both variants of the B1 domain of streptococcal protein G (GB1, 6.2 kDa, pI 4.5) (Gronenborn et al., 1991). The A34F variant forms a simple side-by-side (SBS) kissing-sphere dimer comprising two folded monomers (Jee et al., 2008). The L5V/F30V/Y33F/A34F variant forms a domain-swap (DS) dimer in a reaction involving folding and binding (Byeon et al., 2003; Byeon et al., 2004). These dimers are excellent test systems because, being based on the same protein, they have similar surface chemistries but different association mechanisms.

We quantified the equilibrium thermodynamics of dissociation using ^{19}F nuclear magnetic resonance spectroscopy (NMR) (Chai & Li, 2024; Werle & Kovermann, 2024) because this isotope is 100% abundant. ^{19}F NMR is almost as sensitive as ^{1}H NMR, none of the other solution components contain fluorine, and GB1's sole tryptophan (DS dimer) or its three tyrosines (SBS dimer) are easily labeled with fluorine (Chu et al., 2020, 2022; Crowley et al., 2012; Guseman, Perez Goncalves, et al., 2018; Guseman & Pielak, 2017; Guseman, Speer, et al., 2018; Speer et al., 2021). The labeled residues inhabit different environments in the dimers and monomers. For SBS monomers, only the folded conformation is observed, whereas DS monomers are partially unfolded in buffered solution and progressively adopt a more folded conformation as cosolute concentration increases. In other words, while the cosolutes used here impact only the dimerization of the SBS proteins, these cosolutes can shift both monomer folding and the dimerization of the DS proteins. Both dimers are in slow exchange with their monomers on the fluorine chemical-shift timescale (Byeon et al., 2003; Jee et al., 2008), so the dimer and monomer fractions and the dissociation free energies can be determined from the area under the resonances. Heat capacity changes, enthalpies, and entropies are then determined from the temperature dependence of dimer and monomer fractions.

We chose PEGs and their monomer, ethylene glycol, as cosolutes. The polymers are available in highly pure form at low cost and in many discrete sizes with low polydispersity. Importantly, they are soluble to at least 300 g/L. Although not physiologically relevant, PEGs are used in the pharmaceutical industry and commonly used to study crowding (Speer et al., 2022; Stadmiller & Pielak, 2021). In our experiments, for larger PEGs, concentration crosses from the dilute to the semi-dilute regime (de Gennes, 1979). In the dilute regime, the solvated polymers are sparse, and the polymer chains rarely overlap. The semi-dilute regime is reached at the overlap concentration, c^*, where PEG chains begin to interpenetrate. In this regime the polymer forms a mesh, of characteristic length λ, that partially screens excluded volume interactions (de Gennes, 1979). There are several excellent efforts aimed at understanding the effect of PEGs on the kinetics of protein–protein interactions and dimer formation (Kozer & Schreiber, 2004; Phillip et al., 2009; Stadmiller & Pielak, 2021). Here, we focus on equilibrium thermodynamics.

There are few published efforts aimed at understanding PEG effects on protein complex stability (Stadmiller & Pielak, 2021). The most complete study, by Zosel et al. (2020), investigates the effect of ethylene glycol and 11 PEGs of molecular weight up to 35 kDa and at several concentrations, on the interaction between a disordered- and a molten globule-like protein at a single temperature, 298 K. They report a maximum increased stability of about 1.2 kcal/mol. Stability increases linearly with PEG concentration (g/L), c, at each molecular weight with a slope $(\delta \Delta G'^{o}/\delta c)$ that increases with PEG size. They interpret the stabilization by larger PEGs in terms of depletion interactions (Asakura & Oosawa, 1954; Asakura & Oosawa, 1958) driven by excluded volume. Zhou et al. (2006) studied the effect of 6 kDa and 10 kDa PEGs on the stability of the superoxide dismutase-xanthine oxidase complex using PEG concentrations up to 300 g/L at 298 K. They observe stability increases of 0.4–0.6 kcal/mol and attribute this effect to crowding rather than binding. Furthermore, most studies of protein stability and dimerization by PEGs do not include measurements of enthalpy (Stadmiller & Pielak, 2021), and therefore lack an important source of insight into the underlying mechanism (Speer et al., 2022).

Crowding effects arise from nonspecific interactions, including excluded volume, soft (also called chemical) protein-crowder interactions, and non-ideal mixing (Gnutt et al., 2019; Guseman, Perez Goncalves, et al., 2018; Minton, 2013; Nayar, 2023; Olgenblum et al., 2023; Sapir & Harries, 2015a; Sapir & Harries, 2015b; Sarkar et al., 2013; Schellman, 2003;

Speer et al., 2022; Sukenik et al., 2013; Timr et al., 2020; Xie & Timasheff, 1997; Zhou et al., 2008). The sum of these contributions stabilizes or destabilizes states based on solvent-exposed surface area; they shift the equilibrium between compact states (folded or dimer) and expanded states (unfolded or monomer) (Speer et al., 2022). Excluded volume interactions favor the more compact state—the structured state for protein folding and the dimer for protein–protein interactions (Berg, 1990). Soft interactions can be repulsive or attractive. Repulsive interactions add to the excluded volume and are therefore stabilizing. Attractive soft interactions are destabilizing because they favor the expanded state. The attraction of urea to the protein backbone is an example of a destabilizing small-molecule attractive interaction (Guinn et al., 2013).

Another important, but largely ignored, contribution involves the non-ideal mixing of solvent and cosolute. These interactions affect dimer stability because of the difference in crowder composition near the protein compared to the bulk solution. Upon dimerization, the solvent and crowder near the two monomer interfaces are released into the bulk solution, resulting in mixing. Mixing favors dimerization in the case of attractive non-ideal interactions between components in the solvating solution and favors the monomers when repulsive non-ideal interactions are involved. The combined effect of all interactions can be stabilizing or destabilizing.

Our model for crowding (Sapir & Harries, 2015a) is based on Flory–Huggins theory for binary solutions (Flory, 1942; Huggins, 1942). In the theory, the solvent-cosolute mixing free energy, ΔG_{mix}, is determined by cosolute molecular size and non-ideal solvent-cosolute interactions. Our model considers a ternary mixture of solvent, cosolute, and protein inhabiting two domains: bulk and protein. The bulk domain, which is away from the protein, includes only solvent and cosolutes, so that the thermodynamics are entirely determined by cosolute size and non-ideal interactions. In the protein domain, we also consider soft protein-cosolute interactions. The contributions of these three interactions to dimerization are resolved by fitting the experiment-derived data.

In addition to crowding, cosolutes can specifically bind proteins, which involves precise interactions and recognition between the protein surface and a cosolute ligand (Eriksson et al., 1992; Hermans & Wang, 1997; Niu & Ruotolo, 2015). In many such cases, binding can be characterized by an adsorption equilibrium constant, which typically results in greater stabilization of the bound state compared to what can be achieved through crowding alone (Stewart et al., 2023). For ethylene glycol and PEGs, binding likely involves terminal hydroxyls (Knowles et al., 2015). We find no evidence for the binding of ethylene glycol or PEGs to GB1, and

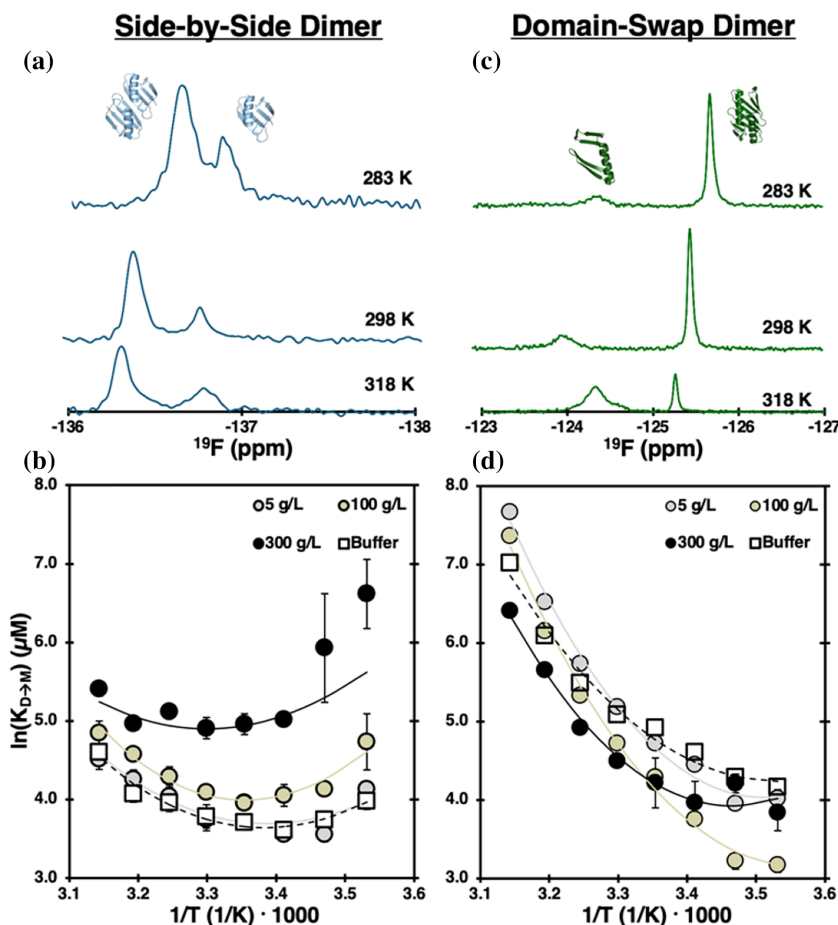therefore analyze the dimer data only in terms of crowding.

We undertook a focused, systematic effort to acquire ^{19}F spectra of the SBS and DS dimers in buffer, ethylene glycol, diethylene glycol, triethylene glycol, and 11 polyethylene glycols up to a molecular weight of 35 kDa (PEG35000), at five concentrations and eight temperatures for each cosolute. We then fit our model to the dissociation thermodynamics of the dimers. For the DS dimer, we account for both folding and association, whereas for the SBS dimer, we consider only association, as its monomers remain folded across all tested PEG concentrations. We find that PEG soft interactions with SBS and DS monomers are attractive, but more attractive toward SBS than DS, explaining the greater destabilization of the SBS dimer by PEGs.

2 | MATERIALS AND METHODS

PEGs were purchased from Sigma-Aldrich and ethylene glycol from Thermo Fisher. 5-Fluoroindole and 3-fluoro-DL-tyrosine were purchased from Thermo Fisher. 5-Fluoroindole is used because it is less expensive than fluorotyrosine. However, we could not use it for the SBS dimer because the dimerization-induced chemical-shift change for the fluoroindole-labeled protein is too small for quantification.

^{19}F-labeled A34F GB1, the SBS dimer, was prepared in BL21 *Escherichia coli* cells as described (Guseman & Pielak, 2017). Briefly, expression was performed in minimal media containing ampicillin and 3-fluoro-tyrosine. After lysis via sonication, the protein was purified using fast protein liquid chromatography, first with an anion-exchange quaternary amine column, and then via size exclusion chromatography. L5V/F30V/Y33F/A34F GB1 (Byeon et al., 2003), the DS dimer, was expressed and purified in the same manner as the A34F variant, except that expression was carried out with 5-fluoroindole instead of 3-fluoro-tyrosine (Crowley et al., 2012; Guseman, Perez Goncalves, et al., 2018). Both variants also contain the T2Q mutation to prevent removal of the N-terminal methionine (Smith et al., 1994). Concentration was quantified spectrophotometrically using ProtParam (Gasteiger et al., 2005) with extinction coefficients at 280 nm of 8470 M^{-1} cm^{-1} for the DS dimer and 9970 M^{-1} cm^{-1} for the SBS dimer.

Spectra were acquired on a Bruker Avance III HD NMR spectrometer equipped with a cryogenic QCI probe containing an H/F channel operating at a ^{19}F Larmor frequency of 470 MHz. Spectra comprised 100 free-induction decays of at least 1024 complex points each, a 30-ppm spectral width, a delay time of 3 s, and an acquisition time of 50 ms. Spectra were subjected to 5-Hz line broadening before zero filling to 262,144 points and Fourier transformation.

Side-by-Side Dimer

(a)

Domain-Swap Dimer

(c)

(b)

(d)

Each dimer gives two ^{19}F resonances: one corresponding to the monomer and the other to the dimer (Figure 1a,c). GB1 has three tyrosines. We used the fluorine resonance from labeled tyrosine 33 to assess the SBS dimer (Guseman & Pielak, 2017). We chose the total protein concentrations for each dimer (SBS, 250 μM; DS, 500 μM) by optimizing the signal-to-noise ratio of spectra and the resolution between monomer and dimer resonances.

For both systems, the monomer and dimer are in slow exchange on the ^{19}F NMR timescale (Byeon et al., 2003; Jee et al., 2008). Therefore, the area under each resonance is proportional to the concentration of the species. Spectra were acquired at eight temperatures (283.15, 288.15, 293.15, 298.15, 303.15, 308.15, 313.15, and 318.15 K), in NMR buffer (20 mM sodium phosphate, 10% D_2O, 0.1% 2,2-dimethyl-2-silapentane-5-sulfonate, pH 7.5), and at a target protein concentration of 250 μM for the SBS dimer and 500 μM for the DS dimer. Crowder solutions were prepared by dissolving the cosolute in NMR buffer, adjusting the pH to 7.5, and diluting to the target concentration with NMR buffer.

The areas of the resonances were used to determine the fraction of dimer (F_d), which, along with

Equation (1), was used to determine the dissociation constant (K_D), where P_t is the total protein concentration.

$$F_d = \frac{4P_t + K_D - \sqrt{K_D + 8P_t K_D}}{4P_t} \quad (1)$$

The free energy of dissociation ($\Delta G'^o_{D\to M}$) was calculated using:

$$\Delta G'^o_{D\to M} = -RT\ln(K_D) \quad (2)$$

The change in free energy of dissociation with crowder concentration compared to buffer ($\Delta\Delta G'^o_{D\to M}$) is given by:

$$\Delta\Delta G'^o_{D\to M}(c) = \Delta G'^o_{D\to M}(c) - \Delta G'^o_{D\to M}(0) \quad (3)$$

where c is crowder concentration and 0 represents a measurement in buffer alone.

The enthalpy of dissociation ($\Delta H'^o_{D\to M}$), was calculated using

$$\ln\left(\frac{1}{K_D}\right) = \frac{1}{K_{D_0}} + \frac{\left(\Delta H'^o{}_{D\to M} - T_0\Delta C_p'^o\right)}{R}\left(\frac{1}{T_0} - \frac{1}{T}\right) \quad (4)$$
$$+ \frac{\Delta C_p'^o}{R}\ln\left(\frac{T}{T_0}\right)$$

where R is the gas constant, T is temperature, $T_o = 298K$ is the reference temperature, and $\Delta C_p'^o$ is the heat capacity of dissociation (Figure S1). Fit examples are in Figure 1b,d. The change in dissociation enthalpy with crowder concentration compared to buffer ($\Delta\Delta H'^o{}_{D\to M}$) is given by:

$$\Delta\Delta H'^o{}_{D\to M}(c) = \Delta H'^o{}_{D\to M}(c) - \Delta H'^o{}_{D\to M}(0) \quad (5)$$

Experiments were conducted at least in triplicate, unless stated otherwise.

The overlap concentration is calculated as: (Lekkerkerker & Tuinier, 2011)

$$c^* = \frac{3M}{4\pi R_g^3 N_A} \quad (6)$$

where M is the molecular mass, N_A is Avogadro's constant, and $R_g = 0.21 \cdot P^{0.583}$ is radius of gyration in nm calculated from the degree of polymerization, P (Zosel et al., 2020).

3 | RESULTS

Both dimers give quantifiable ^{19}F NMR spectra and interpretable van 't Hoff plots (Figure 1b,d); however, the increase in viscosity for larger PEGs at higher concentrations decreases reproducibility, which increases the uncertainty of the thermodynamic parameters. A full list of parameters with uncertainties is provided in the Supplemental Material Data S2 and S3 (DS and SBS spreadsheets).

To investigate the association mechanism, we assessed how PEGs affect ^{19}F chemical shifts and linewidths of the monomers and dimers. Chemical shift changes compared to buffer for the SBS monomer and dimer are small (≤0.27 ppm) and tend to decrease with increasing PEG size and decreasing PEG concentration (Figures S3 and S4). The SBS monomer–dimer linewidth ratio remains approximately constant across all PEG sizes and concentrations, although the ratios are slightly smaller than those in the absence of PEG (Figure 2a). This observation indicates that the change in SBS monomer linewidth relative to its dimer is small and independent of concentration, consistent with the fact that both the SBS dimer and monomer are globular (Jee et al., 2008).

The DS system behaves differently, as evidenced by larger linewidth changes (Figure 2b). Unlike the SBS states, the ratio of monomer-to-dimer linewidth decreases with increasing cosolute concentration in a manner nearly independent of cosolute molecular weight. Moreover, the change in monomer chemical shift compared to buffer varies three times more than it does for the SBS monomer and dimer (Figures S3 and S4) but dimer shifts are unaffected. These observations are consistent with the fact that in buffer the monomer of the DS dimer is only partially folded (Byeon et al., 2003) and suggest that PEGs favor a more compact monomeric state, but the folded dimer is unaffected.

The DS monomer is partially folded in buffer (Byeon et al., 2003; Byeon et al., 2004) and folds in the presence of the cosolutes used here. We assume that the structures of the SBS dimer, its monomer, and the DS dimer do not change with temperature over the range studied, cosolute size, or cosolute concentration. This assumption is reasonable for the SBS dimer and monomer because both are stable and globular (Jee et al., 2008), and we have indirect evidence that the same is true for the DS dimer. Specifically, the linewidth of the DS dimer increases linearly with increasing viscosity of PEG 400 solutions, as does the SBS dimer (Figure S5). Interpreted in terms of the Stokes–Einstein–Debye equation (Debye, 1929; Einstein, 1956), the simplest explanation of these observations is that the dimer radii are unchanged in PEG, and their linewidths increase because of increased viscosity.

FIGURE 2 Ratio of ^{19}F NMR linewidths comparing monomer to dimer for EG, PEG 1 kDa, and PEG 35 kDa at 298 K for the (a) SBS dimer and the (b) DS dimer. The ratio is the full width at half height of the monomer divided by that of the dimer. Error bars represent the standard error of the mean from triplicates.
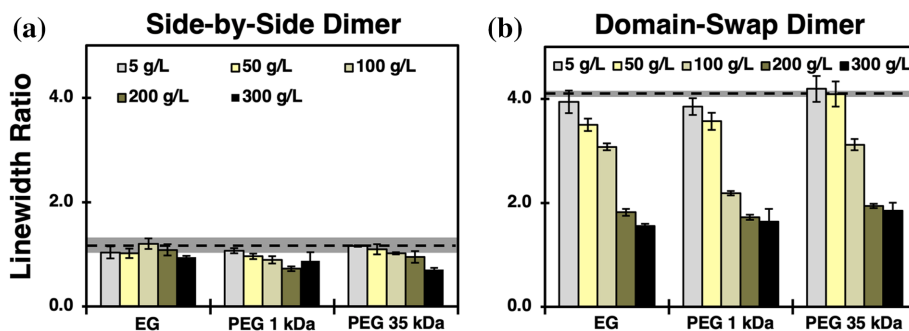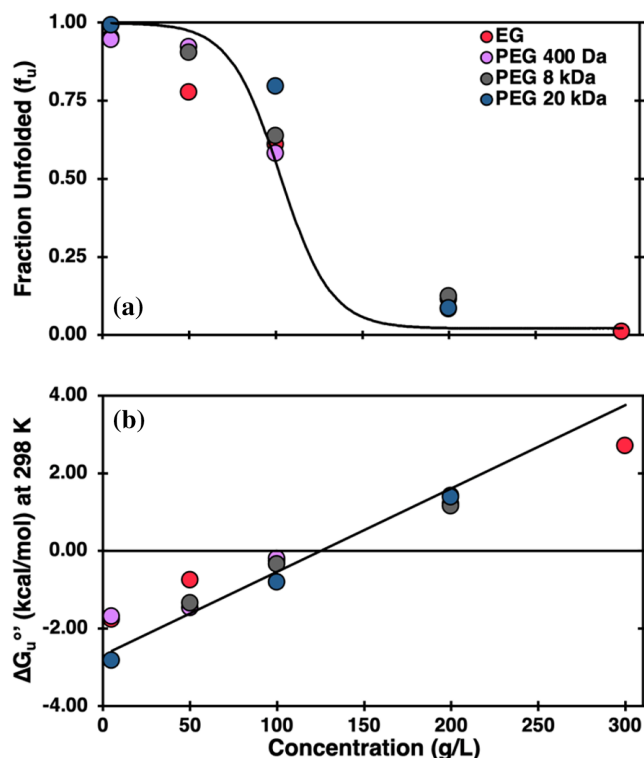
FIGURE 3 DS monomer folding. (a) Fraction of unfolded DS monomer as a function of cosolute concentration. Fraction partially folded was determined using the ^{19}F NMR linewidth ratios. (b) Free energy of unfolding for the DS monomer as a function of cosolute concentration. Free energies were calculated using linear least squares analysis in Excel and extrapolating to the y-intercept.

We followed compaction of the DS monomers by analyzing the linewidth ratios (Figure 2b) assuming a two-state reaction between the partially- and fully folded monomer. This assumption allowed us to determine the fraction of partially unfolded monomers, f_u, within the entire monomer population as it relates to the linewidth ratio, L_{obs}, and the limiting linewidth ratios of the folded, L_f, to the partially unfolded, L_u, monomers via $L_{obs} = f_u L_u + (1 - f_u)L_f$ for EG, PEG400, PEG8000, and PEG20000. f_u, like the linewidth ratios, is independent of PEG size (Figure 3a). The corresponding monomer unfolding free energies, $\Delta G'^o_u$ (Figure 3b), were calculated using Equation (2), where the equilibrium constant is $K_u = f_u/(1 - f_u)$. Our two-state assumption is valid because the data show the expected (Wyman, 1964) linear dependence of unfolding free energy on cosolute concentration (Figure 3b). Other PEGs show the same behavior (Figure S6), but we chose to show only those data with a <5% chance of arising from uncorrelated data (Figures 3 and S7). We conclude that the monomers of the DS dimer undergo a two-state transition from a partially folded ensemble at concentrations up to 50 g/L to a fully folded state at concentrations above 200 g/L. $\Delta G'^o_u$ at 298 K changes from approximately −2 kcal/mol at 5 g/L, indicating a

preponderance of the partially unfolded monomer, to +2 kcal/mol at 300 g/L, indicating a majority of folded monomer.

We followed dimer stability using $\Delta\Delta G'^o_{D\to M}$, determined using Equations (1) and (2). Contrary to predictions of simple crowding theory, PEGs and ethylene glycol tend to decrease $\Delta\Delta G'^o_{D\to M}$, so that the cosolutes destabilize the dimers compared to buffer (Figure 4a,c). Also contrary to simple crowding model predictions, PEGs affect $\Delta\Delta H'^o_{D\to M}$, generally decreasing it compared to buffer (Figure 4b,d). The negative sign corresponds to a destabilizing contribution to dimerization. PEGs, however, do not affect the heat capacity of dissociation in a statistically significant way (Figure S1).

Smaller PEGs and ethylene glycol are most destabilizing (Figures 4a,c and S2). The trend is concentration dependent, with higher concentrations being more destabilizing. The dissociation free energies of the SBS dimer show a monotonic trend, whereas for the DS dimer, they are divided into two distinct regimes that transition around 150 g/L and whose emergence is more pronounced as PEG size increases (Figures 4c and S2). The regimes correspond to dimerization of the partially folded monomer ensemble at low concentrations and dimerization of folded monomer at high concentrations, implying that the impact of folding of the DS monomers is evidenced in $\Delta\Delta G'^o_{D\to M}$. For the SBS dimer, destabilization plateaus at about 500 Da PEG at all concentrations, and for the DS dimer, destabilization vanishes ($\Delta\Delta G'^o_{D\to M} \approx 0$) for PEGs above about 500 Da (Figures 4c and S2).

Cosolutes tend to decrease the enthalpy of dissociation of both dimers (Figures 4b,d and S2). $\Delta\Delta H'^o_{D\to M}$ of the SBS dimer decreases monotonically, but does not converge smoothly to buffer values from data measured between 50 to 300 g/L. To verify that $\Delta\Delta H'^o_{D\to M}$ extrapolates to buffer values we acquired data for the SBS dimer at concentrations below 5 g/L. These data, along with the higher concentration data for the SBS dimer are shown using a logarithmic concentration scale (Figure 4b, inset), indicating that $\Delta\Delta H'^o_{D\to M}$ approaches the buffer value at low PEG concentrations. The enthalpy change at 50 to 300 g/L compared to the enthalpy change in the absence of PEG is independent of PEG size, and approximately constant with PEG concentration. This constant contribution is associated with a slight compaction of the SBS monomer even at 5 g/L PEG and can be seen in the slight reduction in the SBS dimer-monomer linewidth ratio upon adding PEG (Figure 2a).

Like the SBS dimer, $\Delta\Delta H'^o_{D\to M}$ for the DS dimer does not appear to converge, showing a "hump" but at a higher concentration than the SBS dimer. That is, the same distinct regimes are seen in $\Delta\Delta G'^o_{D\to M}$ and $\Delta\Delta H'^o_{D\to M}$. The enthalpic trend with size is hardly

FIGURE 4 Dissociation free energies of (a) SBS- and (c) DS- dimers, and dissociation enthalpies of (b) SBS- and (d) DS- dimers at 298 K as a function of crowder concentration. Insets in panels a and b show data as a function of log concentration. Error bars represent the standard error of the mean from triplication (except for 0.002 g/L PEG 400 Da, which is from duplication). Points in the insets for cosolute concentrations <1 g/L represent a single trial. The dashed line represents the buffer value and the shading its standard deviation of the mean.
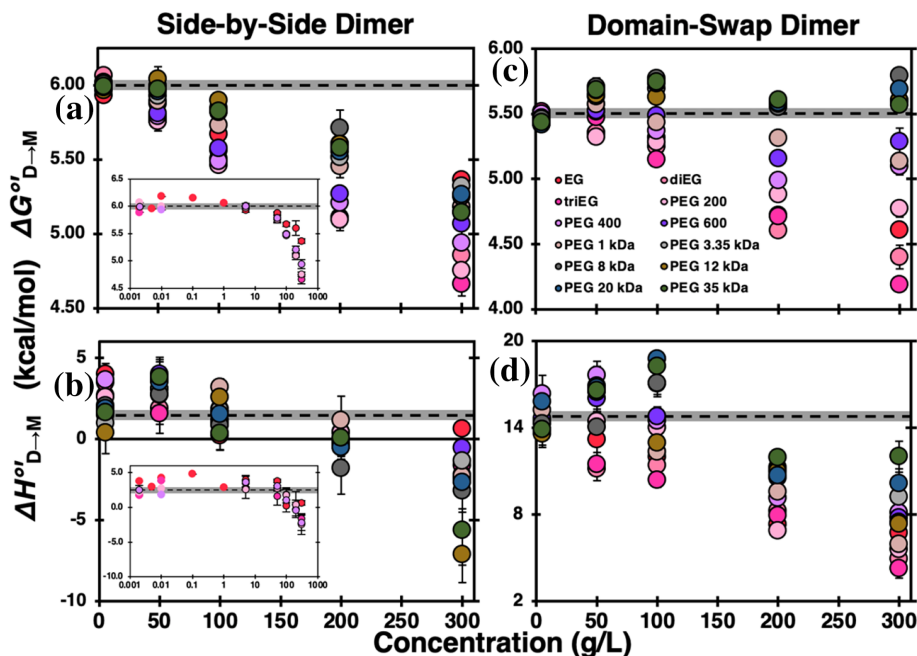
resolved, but the decrease is more pronounced at higher cosolute concentrations (Figure S2).

In summary, crowding by PEGs tends to destabilize both dimers, although there is a small stabilizing effect for the DS dimer in higher molecular weight PEGs. For smaller PEGs, destabilization tends to be enthalpically driven, except at low PEG concentrations where the enthalpy is stabilizing due to changes in the monomer ensemble.

4 | DISCUSSION

4.1 | Mean-field model dissects cosolute interactions

We employ our model (Sapir & Harries, 2015a) to analyze the thermodynamic mechanism underlying protein dimerization in aqueous solutions of PEGs. In the model, changes in dimer stability arise from exclusion or inclusion of cosolutes at the exposed surface of the unbound monomers that are buried in the dimer (Sapir & Harries, 2015b). Exclusion stabilizes the dimer compared to the monomer. Conversely, cosolute inclusion at the larger exposed interface of the monomer (relative to the dimer) leads to dimer destabilization. We neglect explicit cosolute-GB1 binding for monomers and dimers due to lack of evidence.

Our approach extends Flory–Huggins theory for binary solvent-polymer mixtures (Flory, 1942; Huggins, 1942) to ternary mixtures that include proteins. The solution is divided into bulk and protein domains. The bulk domain is far away from the protein. That is, cosolutes in the bulk solution do not interact

with the protein. The protein domain encompasses a volume of thickness α from the protein, within which cosolutes can interact with the protein. We set a as the typical linear dimension of the cosolute molecule. For polymeric crowders at or above the overlap concentration, c^*, α generally decreases with increasing crowder concentration due to inter-chain penetration. For small cosolutes like ethylene glycol, sugars, polyols, and other organic osmolytes, α is constant, reflecting their molecular size.

The model accounts for three types of interactions, each representing a phenomenological parameter: excluded volume (ν), non-ideal solvent-cosolute mixing (χ), and soft protein-cosolute (ε) interactions. Unlike ν and χ, which are measured in the absence of protein, ε manifests exclusively in the protein domain and is protein specific. We have derived values of ν and χ for ethylene glycol and PEGs (Stewart et al., 2023). Values of ν, the ratio between cosolute- and the solvent- partial molar volumes $\overline{V}_C/\overline{V}_S$, changes linearly with PEG size (Figure S8). Values of χ, derived from aqueous PEG water activity measurements, exhibit two distinct regimes: $\chi \approx 0.3$ for ethylene glycol and small PEGs and $\chi \approx 0.4$ for PEGs beyond ∼PEG1000 (Figure S9).

The enthalpic and entropic contributions to χ, χ_H and χ_{TS}, are derived from the temperature dependence of water activities by using the van 't Hoff relation, $\partial \chi/\partial T^{-1} = T\chi_H$ and $\chi_{TS} = \chi_H\text{-}\chi$. The entropic contribution values, χ_{TS}, decrease with PEG size, except for ethylene glycol, which exhibits the lowest value (Figure S10). We determined ε for the interactions of the dimers with PEGs by fitting the experiment-derived $\Delta\Delta G'^{o}_{D\rightarrow M}$ values. Detailed model information is

provided in the Supporting Information, and an implementation of the code is available (Olgenblum, 2023).

An asset of our model is its ability to differentiate each type of free energy contribution, thereby elucidating the crowding mechanism. For example, our model shows that the stabilization of an SH3 domain by large PEGs is driven by excluded volume interactions and exothermic non-ideal mixing of PEG and water upon folding (Stewart et al., 2023). Direct SH3-PEG soft interactions are negligible for larger PEGs. Conversely, the model reveals that soft interactions are significant for small cosolutes such as polyols and sugars, and that they can be stabilizing for one protein yet destabilizing for another, even for the same cosolute (Olgenblum et al., 2023).

4.2 | PEG-induced dimer destabilization increases at high PEG concentrations because mesh size, λ, decreases

Fitting the SBS and DS data proceed differently, because the SBS monomers remain folded and only dimerize, while the DS monomers both fold and dimerize (Figure 5).

Fitting proceeds in two steps for SBS dimerization. First, we fit the experiment-derived $\Delta\Delta G'^{o}_{D\to M}$ values in the presence of small crowders, ranging from ethylene glycol to PEG200, using ε as the only fit parameter. We set $\alpha = \nu^{1/3}$ because the size of the small crowders is independent of their concentration (i.e., they are too small to form a mesh). For the larger PEGs, ε should not depend strongly on PEG size, because most PEG-protein interactions originate from the repeating moieties of PEG rather than its ends, and the ends are at low concentration for large PEGs even at high PEG concentrations. Therefore, in the second step, we use

the limiting value of ε from the small PEGs as described above and fit $\Delta\Delta G'^{o}_{D\to M}$ using a as the only fit parameter. In all fits, we use the values of ν and χ derived from measurements of binary mixtures.

For DS dimerization, we must account for PEG-induced monomer folding, which primarily contributes to $\Delta\Delta G'^{o}_{D\to M}$ at low concentrations. Above $\sim$200 g/L, most monomers are folded, so that only dimerization contributes to the free energy. The dissociation free energy is therefore given by $\Delta\Delta G'^{o}_{D\to M} = \Delta\Delta G'^{o}_{D\to f} + f_u \cdot \Delta\Delta G'^{o}_{f\to u}$, where $\Delta\Delta G'^{o}_{D\to f}$ is the change in the free energy of the dimer dissociating into the folded monomers and $\Delta\Delta G'^{o}_{f\to u}$ is the unfolding free energy of the DS monomers, which is scaled by f_u to account for the unfolded fraction. In the limit of $f_u \to 1$, $\Delta\Delta G'^{o}_{f\to u}$ fully contributes because all the monomers partially unfold upon dissociation. Conversely, in the limit of $f_u \to 0$, there is no contribution from $\Delta\Delta G'^{o}_{f\to u}$, as all monomers remain folded. In the fitting procedure f_u is determined from the global fit of the experimentally derived fraction of partially unfolded monomers in each cosolute (Figure 2b). We determine $\Delta\Delta G'^{o}_{D\to f}$ and $\Delta\Delta G'^{o}_{f\to u}$ for the small crowders simultaneously by fitting the soft interaction parameters associated with dissociation, ε, and unfolding, ε_u, while setting $a = \nu^{1/3}$. For the larger PEGs, we set the values of ε and ε_u to the limiting value obtained for small PEGs and fit $\Delta\Delta G'^{o}_{D\to M}$ using a as the only fit parameter.

The change in protein domain size, a, with PEG concentration (Figure 6a,b) indicates that a decreases with concentration for PEGs larger than 200 Da for both dimers. The decrease in a with concentration is more pronounced for larger PEGs. This observation is explained by the expected variation of PEG mesh size, λ, which is the relevant length scale in the semi-dilute regime (Sorichetti et al., 2020; Zosel et al., 2020). This conclusion seems to be general because λ is also the
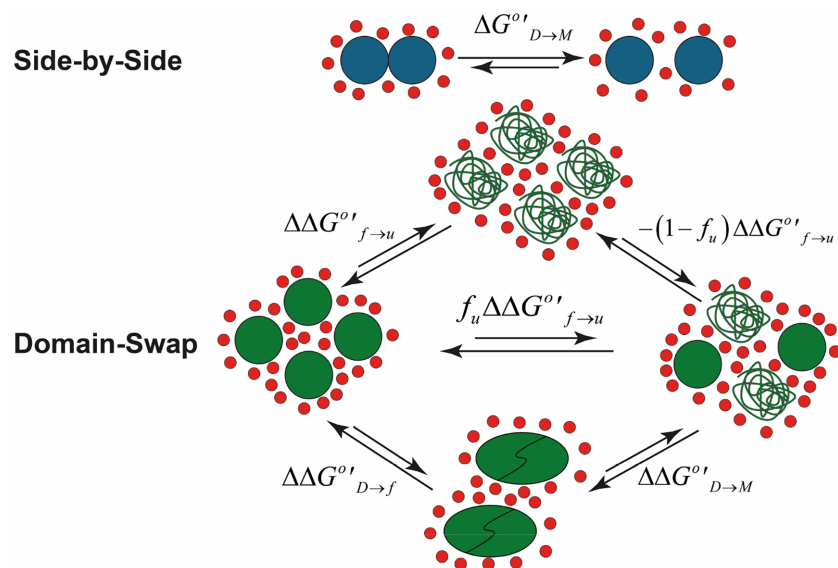

FIGURE 5 Mechanism of SBS (blue) and DS (green) dimerization in presence of PEGs. Large circles represent folded monomers, strings represent partially folded monomers. Small red circles represent PEGs. The SBS dimer is represented as kissing circles. The DS dimer is represented as an oval. Relative arrows sizes indicate the free energy changes for large PEGs.

FIGURE 6 Log–log plots of protein domain size (α) relative to water (α_s, 3 Å) against normalized mass concentration relative to c^* and the slopes of those lines (ξ) versus crowder size for the (a, c) SBS and (b, d) DS dimers, at 298 K. Gray horizontal lines in panels (c) and (d) represent the slope for de Gennes scaling exponent.
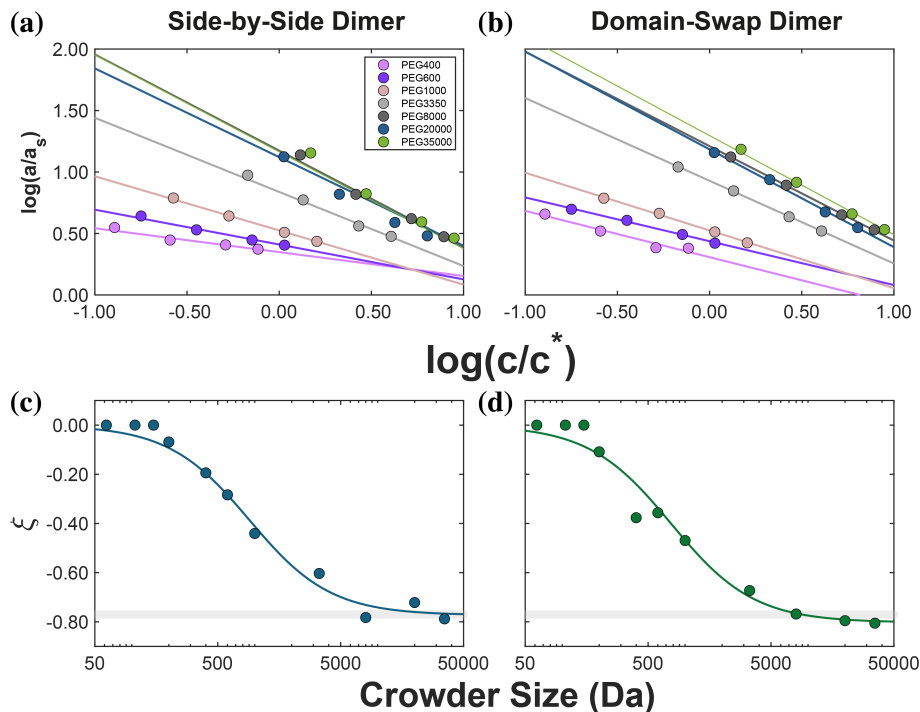
FIGURE 7 Fits to changes in dissociation free energy for the (a–c) SBS- and (d–f) DS- dimers at 298 K: (a, d) Ethylene glycol, and small crowders, (b, e) medium PEGs, and (c, f) large PEGs. Circles represent experiment-derived values. Insets show contributions of $\Delta\Delta G'^{o}_{D\to f}$ and $\Delta\Delta G'^{o}_{f\to u}$ to the $\Delta\Delta G'^{o}_{D\to M}$ of DS dimer.
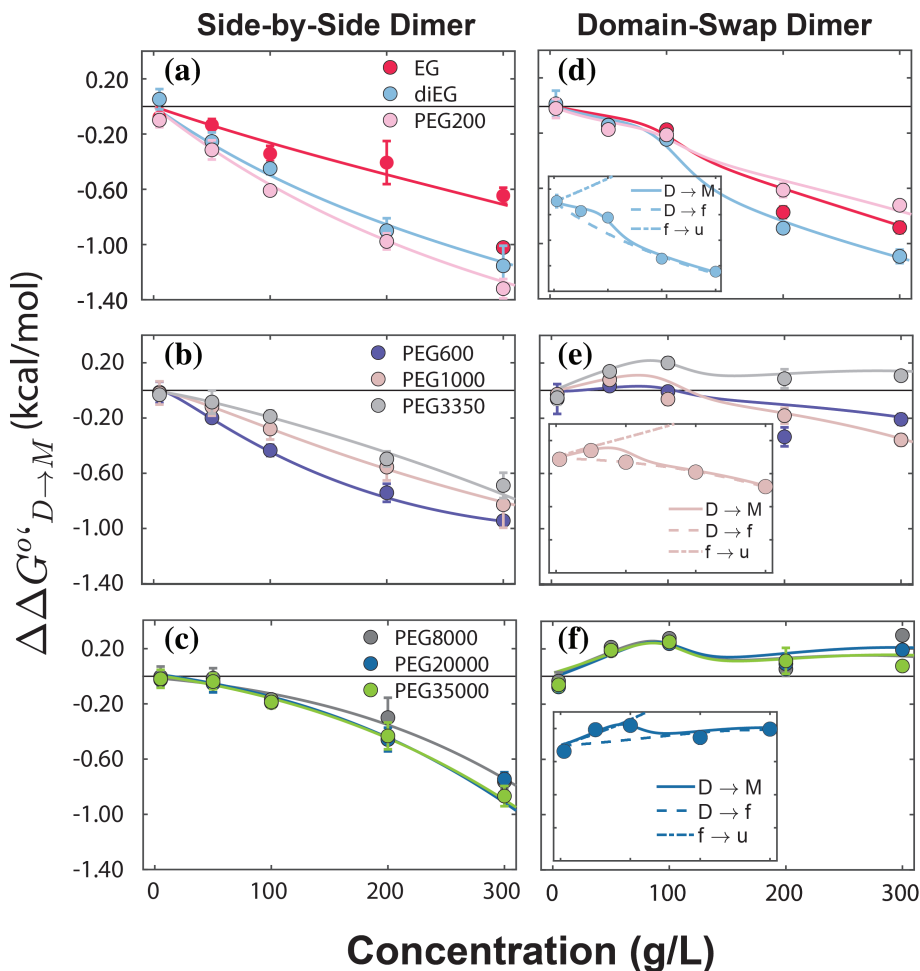
relevant length scale for SH3 folding in PEG solutions (Stewart et al., 2023). The decrease in a with increasing concentration mitigates the impact of excluded volume and non-ideal mixing, because both effects scale with protein domain volume. The relative impact of destabilizing protein-PEG soft interactions increases, because soft interactions scale with protein surface area. The result is greater destabilization due to the decrease in a with PEG concentration.

For a polymer chain in a good solvent, like PEG in water (Devanand & Selser, 1991), the mesh size should follow the de Gennes scaling law, $\lambda \sim R_g(c/c^*)^\xi$ (de Gennes, 1979), with exponent $\xi = -0.77$. The corresponding exponent for PEG in our model is given by $\xi = \mathrm{d}\log(\alpha/\alpha_s)/\mathrm{d}\log(c/c^*)$. As PEG size increases, ξ decreases from 0 (corresponding to no concentration dependence of α) to the de Gennes scaling exponent (Figure 6c,d). The transition between these limits is sigmoidal.

## 4.3 | PEGs interact more strongly with SBS monomers than with DS monomers

Fits of $\Delta\Delta G'^o_{D\to M}$ versus crowder concentration for the dimers (Figure 7) show that the model accounts for data across all PEG sizes for both dimers. The dissociation of the DS dimer involves opposing PEG contributions: $\Delta\Delta G'^o_{D\to f}$ is destabilizing, whereas $\Delta\Delta G'^o_{f\to u}$ is stabilizing (Figure 7d, inset).

ε is negative for both dimers in all PEGs (Figure 8a), suggesting that dimer destabilization arises from PEG-protein attraction, which leads to PEG being preferentially included at the exposed surfaces of the monomers. These surfaces are buried in the dimer; dimerization strips the surface of excess (favorably interacting) PEG, which stabilizes the monomer compared to the dimer. Except for ethylene glycol, ε is more negative for the SBS dimer than the DS dimer, which explains the greater destabilization of the SBS dimer (Figure 7). The difference of 0.04 in value of ε for PEGs with SBS compared to the DS dimer corresponds to 0.25 kcal mol^{-1} nm^{-2}. This surplus attraction to the globular monomers of the SBS dimer is linked to the greater stability of these monomers compared to the marginally stable, partially folded, DS monomers. That is, the monomers of the DS dimer collapse and fold on adding cosolutes. Folding reduces the opportunity for protein-PEG attraction. Surprisingly, ε_u does not vary monotonically with PEG size (Figure 8b), remaining approximately zero for both small and large PEGs, but becoming negative for intermediate-sized PEGs, slightly reducing the stabilizing effect of excluded volume interactions for these cosolutes.

4.4 | Enthalpic (soft) protein-PEG interactions are destabilizing

Our model dissects the dissociation free energy into contributions from excluded volume, $\Delta\Delta G'^o_\nu$, non-ideal mixing, $\Delta\Delta G'^o_\chi$, and soft-interactions, $\Delta\Delta G'^o_\varepsilon$, in addition to the contribution associated with folding the DS monomers, $\Delta\Delta G'^o_{f\to u}$. The main contribution to dimer destabilization is $\Delta\Delta G'^o_\varepsilon$ (Figure 9, blue curves), which is negative for all crowders at all concentrations. For ethylene glycol, PEG600, and PEG8000, $\Delta\Delta G'^o_\nu$ is, as expected, always positive (i.e., stabilizing, red curves). By contrast, $\Delta\Delta G'^o_\chi$ (green curves) is approximately
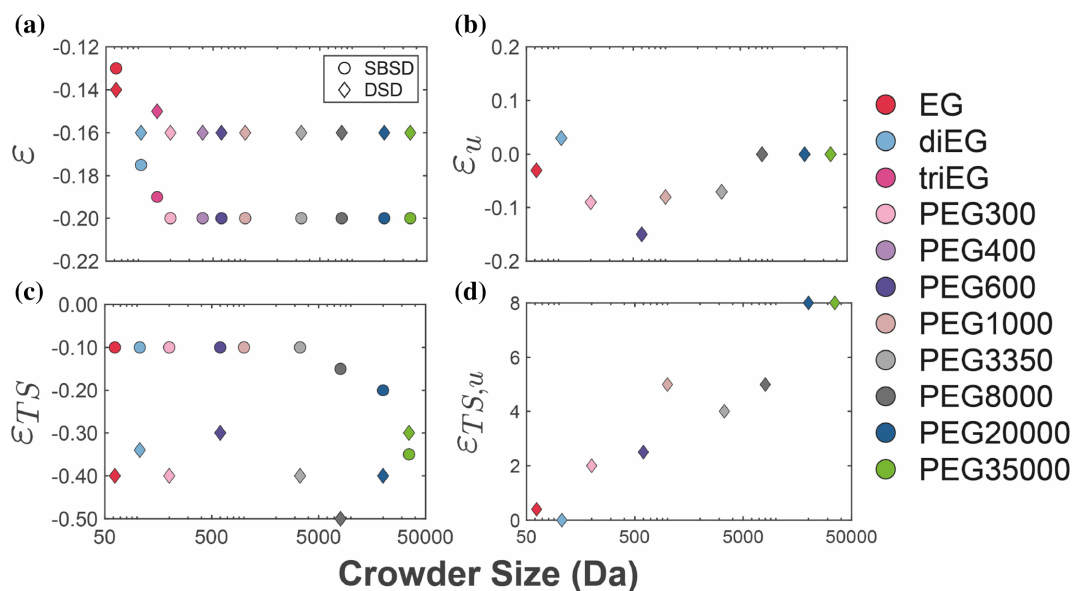
FIGURE 8 Soft interaction parameters of PEGs associated with (a) dimerization and (b) folding, and the entropic contribution of soft interactions to (c) dimerization and (d) folding. ε is the interaction free energy given in RT per exposed protein area in terms of as 2, at T0 = 298K.
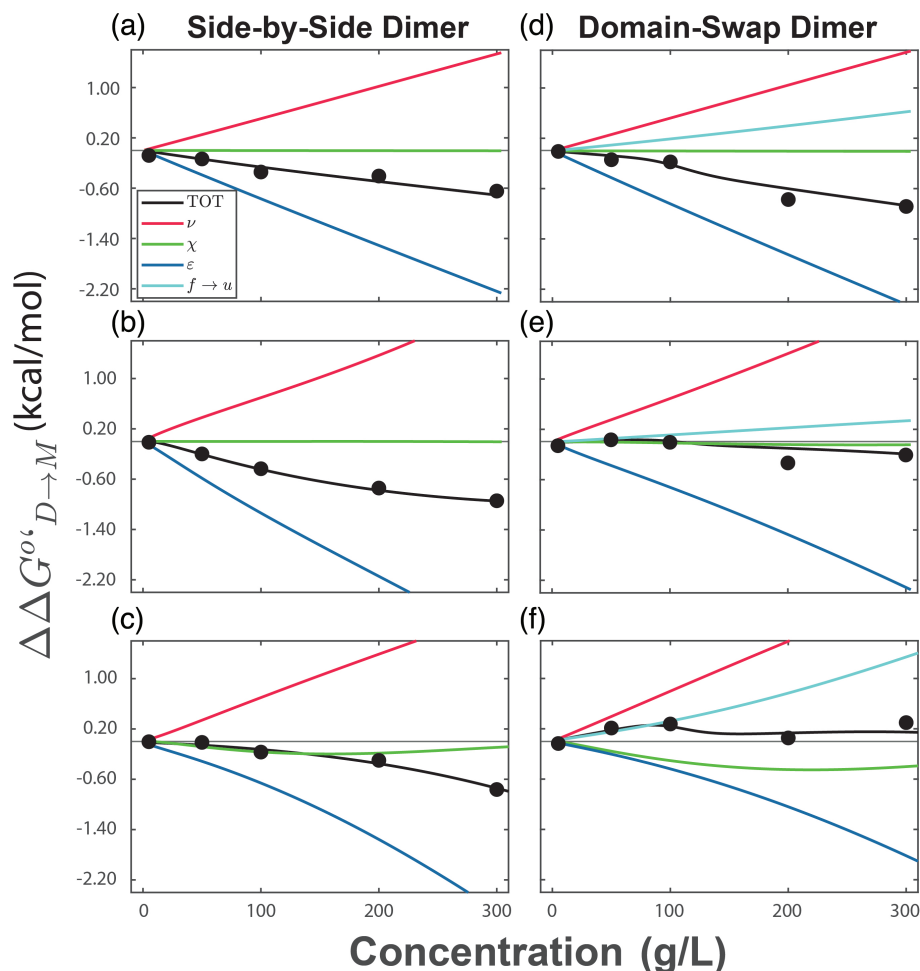
zero for small and medium cosolutes and slightly negative for larger PEGs, and therefore mildly destabilizing, as required by the positive values of χ.

To understand the origins of enthalpic and entropic contributions, we fit the model to the $\Delta\Delta H'^0_{D \rightarrow M}$ and $T\Delta\Delta S^{0\prime}_{D \rightarrow M}$ data. The dissociation and unfolding soft interaction parameters are resolved into their enthalpic and entropic components, $\varepsilon = \varepsilon_H - \varepsilon_{TS}$ and $\varepsilon_u = \varepsilon_{H,u} - \varepsilon_{TS,u}$, respectively. For the DS dimer we consider both dissociation and unfolding so we fit ε_{TS} and $\varepsilon_{TS,u}$. By contrast, for the SBS dimer we consider only dissociation, and accordingly only ε_{TS} needs to be determined. Note that ε_{TS} and $\varepsilon_{TS,u}$ are the only fit parameters because ε, ε_u, and a are already determined from fits to $\Delta\Delta G'^0_{D \rightarrow M}$.

For the SBS dimer, fits to $\Delta\Delta H'^0_{D \rightarrow M}$ as a function of concentration for ethylene glycol and a range of PEG sizes (Figure 10) are monotonic because, unlike the monomers of the DS dimer, SBS monomers remain folded between 50 and 300 g/L. The fits of $\Delta\Delta H'^0_{D \rightarrow M}$ converge to ≈ 1.9 kcal/mol instead of zero, probably because of an additional enthalpy associated with the slight compaction of the SBS monomer below 5 g/L (Figure 2a). For the DS dimer, our model fits the non-monotonic $\Delta\Delta H'^0_{D \rightarrow M}$, even the peak at ≈ 100 g/L,

which results from the sum of the positive $\Delta\Delta H'^0_{f \rightarrow u}$ and negative $\Delta\Delta H'^0_{D \rightarrow f}$ (Figure 10d–f, insets).

Finally, we consider ε_{TS} and $\varepsilon_{TS,u}$ (Figure 8c,d). For both proteins ε_{TS} is negative for all PEGs, meaning that the entropic contribution to the soft interactions is stabilizing. ε_H is also negative, suggesting that destabilization arises from enthalpic protein-PEG chemical interactions. Like the free energies, the enthalpic and the entropic contributions with the same PEGs differ between the proteins. $\varepsilon_{TS} \approx -0.35$ remains approximately constant for the SBS dimer with all PEGs, whereas for the DS dimer ε_{TS} remains at -0.1 from ethylene glycol up to PEG3350 and becomes more negative as the size of PEG increases from PEG8000 onwards. Although PEG is attracted more strongly to the SBS- than the DS-monomers, attraction to the SBS monomers involves smaller enthalpic and entropic contributions compared to those for the DS monomers, meaning there is less enthalpy-entropy compensation for the SBS dissociation. Although the enthalpic contribution to the soft interactions is more attractive for the DS dimer, the large stabilizing entropic contribution for the DS dimer strongly compensates, leading to overall greater protein-PEG attraction for the SBS dimer.
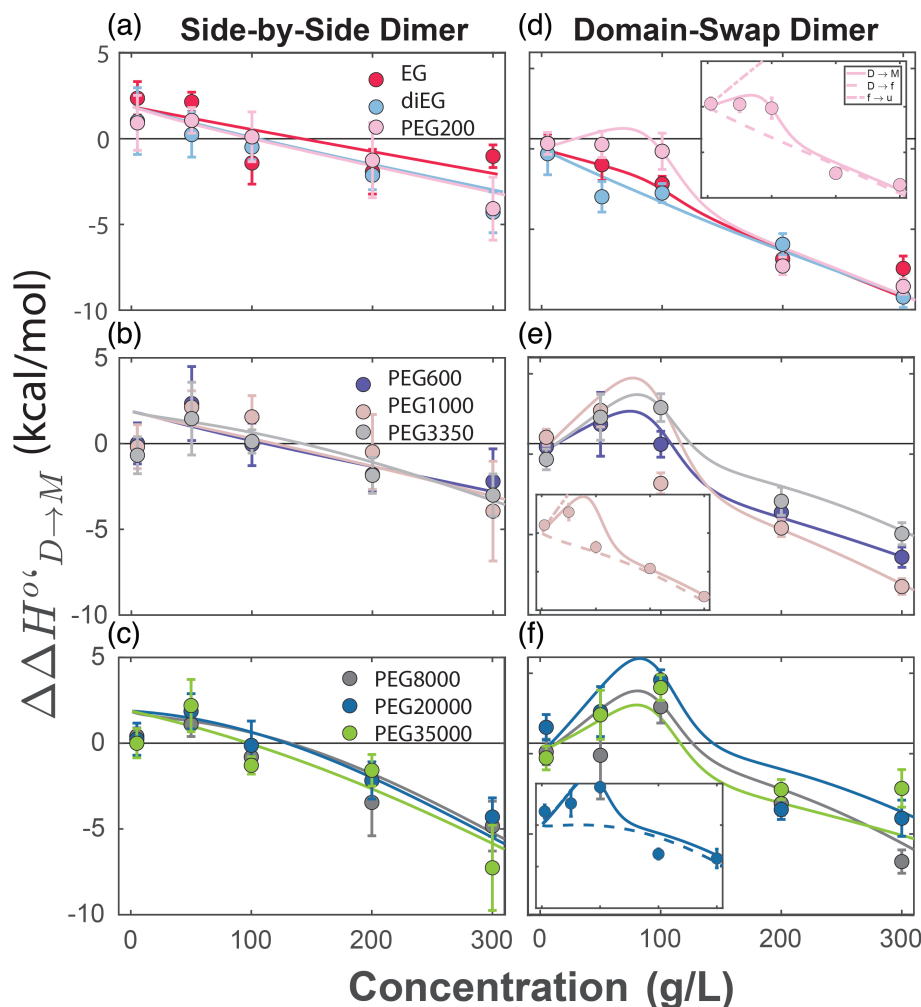
FIGURE 10 Fits to enthalpy data for the (a–c) SBS and (d–f) DS dimers at 298 K: (a, d) Ethylene glycol, and small crowders, (b, e) medium PEGs, and (c, f) large PEGs. Circles represent experiment-derived values. Insets show contributions of $\Delta\Delta G'^{o}_{D\to f}$ and $\Delta\Delta G'^{o}_{f\to u}$ to the $\Delta\Delta G'^{o}_{D\to M}$ of DS dimer.

Unlike ε_{TS}, $\varepsilon_{TS,u}$ increases monotonically with PEG size from ≈ 0 to ≈ 8, suggesting that the enthalpy and entropy associated with soft interactions for unfolding are strongly compensating, with enthalpy strongly destabilizing.

5 | CONCLUSIONS

We followed the dissociation of two protein dimers with similar surface chemistry but different association mechanisms as a function of PEG size, PEG concentration and temperature. Using our model we deconvoluted the excluded volume, non-ideal mixing, and soft interactions contributing to the equilibrium thermodynamics using only a small set of parameters, namely the soft interaction parameter, ε, and the protein domain thickness, a. By accounting for the change in a with cosolute concertation, our model captures the polymeric nature of PEGs, the de Gennes scaling exponent. Importantly, the exponent emerges from the fits to the model but is not part of the model. That is, our model predicts de Gennes scaling, highlighting the robust nature of our approach. The decrease in mesh

size weakens excluded volume interactions, thereby increasing destabilization by soft interactions.

Analysis of the ^{19}F-NMR line widths shows that the size of the SBS monomers is almost unaffected by PEG, whereas DS monomers fold as the cosolute concentration increases. This change in the monomer ensemble, from partially folded to folded, manifests in the dissociation free energies and enthalpies. We account for folding, in addition to dissociation, by employing a simple thermodynamic cycle (Figure 5), which we fit to our experimentally derived free energies and enthalpies.

The fits show that cosolute-induced dimer destabilization mainly arises from the attractive soft interactions of PEGs with the monomer interface. The SBS dimer is more destabilized than the DS dimer because PEG interacts more strongly with the SBS monomer than the DS monomer. For both dimers, these attractive protein-PEG soft interactions are enthalpic, suggesting that PEG's repeating moieties favorably interact with the monomer interface, destabilizing the dimer. Although the enthalpic contribution to the soft interactions is more attractive for the DS dimer, its large repulsive entropic contribution strongly compensates, leading to greater protein-PEG destabilization for the SBS dimer.

In addition to their nonspecific attractive interactions with the protein, large PEGs are destabilizing through their non-ideal mixing, which intensifies as solvent is released upon dimerization. This destabilizing contribution augments the ideal mixing term in solvent release that favors the dimers. This contribution is negligible for small PEGs because non-ideality increases with polymer size. Lastly, folding of the DS monomers by PEG stabilizes the dimer at low cosolute concentrations, where the fraction of partially folded monomers is nonzero. At high cosolute concentrations, all the monomers are folded, so that the addition of PEG acts only by crowding the folded monomers and dimers. Folding is driven by enthalpy because of PEG's enthalpic repulsion from the surface of the partially folded monomers.

Our work illuminates the effects of crowding on protein dimer dissociation. The conclusions represent an important step toward understanding protein–protein interactions in complex, biologically relevant environments. The comprehensive foundation provided here is essential for deciphering the molecular mechanisms crucial to forming the protein complexes that play vital roles in cells.

AUTHOR CONTRIBUTIONS

Gil I. Olgenblum: Investigation; formal analysis; writing – original draft; writing – review and editing; software; visualization. **Claire J. Stewart:** Conceptualization; methodology; formal analysis; supervision; visualization; writing – review and editing; investigation; data curation. **Thomas W. Redvanly:** Investigation; writing – original draft; writing – review and editing; formal analysis; data curation; visualization. **Owen M. Young:** Investigation; writing – original draft; writing – review and editing; formal analysis; data curation; methodology; visualization. **Francis Lauzier:** Investigation; formal analysis; writing – review and editing; methodology. **Sophia Hazlett:** Investigation; writing – review and editing; formal analysis. **Shikun Wang:** Investigation; writing – review and editing; formal analysis. **David A. Rockcliffe:** Investigation; writing – review and editing; formal analysis. **Stuart Parnham:** Supervision; investigation; resources. **Gary J. Pielak:** Conceptualization; methodology; supervision; resources; project administration; writing – review and editing; writing – original draft; funding acquisition; formal analysis. **Daniel Harries:** Conceptualization; methodology; supervision; project administration; funding acquisition; writing – original draft; writing – review and editing; formal analysis.

ACKNOWLEDGMENTS

CONFLICT OF INTEREST STATEMENT

The authors declare no conflicts of interest.

DATA AVAILABILITY STATEMENT

All data are included in the manuscript and/or supporting information.

ORCID

Gil I. Olgenblum https://orcid.org/0000-0002-4514-5516
Gary J. Pielak https://orcid.org/0000-0001-6307-542X
Daniel Harries https://orcid.org/0000-0002-3057-9485

REFERENCES

Asakura S, Oosawa F. On interaction between two bodies immersed in a solution of macromolecules. J Chem Phys. 1954;22:1255–6.

Asakura S, Oosawa F. Interaction between particles suspended in solutions of macromolecules. J Polym Sci. 1958;33:183–92.

Berg OG. The influence of macromolecular crowding on thermodynamic activity: solubility and dimerization constants for spherical and dumbbell-shaped molecules in a hard-sphere mixture. Biopolymers. 1990;30:1027–37.

Byeon I-JL, Louis JM, Gronenborn AM. A protein contortionist: Core mutations of GB1 that induce dimerization and domain swapping. J Mol Biol. 2003;333:141–52.

Byeon I-JL, Louis JM, Gronenborn AM. A captured folding intermediate involved in dimerization and domain-swapping of GB1. J Mol Biol. 2004;340:615–25.

Chai Z, Li C. In-cell ^{19}F NMR of proteins: recent progress and future opportunities. Chem A Eur J. 2024;30:e202303988.

Chu IT, Speer SL, Pielak GJ. Rheostatic control of protein expression using tuner cells. Biochemistry. 2020;59:733–5.

Chu I-T, Stewart CJ, Speer SL, Pielak GJ. A difference between *in vitro* and in-cell protein dimer formation. Biochemistry. 2022;61:409–12.

Crowley PB, Kyne C, Monteith WB. Simple and inexpensive incorporation of ^{19}F-tryptophan for protein NMR spectroscopy. Chem Commun. 2012;48:10681–3.

de Gennes P-G. Scaling concepts in polymer physics. Ithaca, NY: Cornell University Press; 1979.

Debye PJ. Polar molecules. New York: Chemical Catalog Company; 1929.

Devanand K, Selser JC. Asymptotic behavior and long-range interactions in aqueous solutions of poly(ethylene oxide). Macromolecules. 1991;24:5943–7.

Einstein A. Investigations on the theory of the Brownian movement. New York: Dover Publications; 1956.

Eriksson AE, Baase WA, Wozniak JA, Matthews BW. A cavity-containing mutant of T4 lysozyme is stabilized by buried benzene. Nature. 1992;355:371–3.

Flory PJ. Thermodynamics of high polymer solutions. J Chem Phys. 1942;10:51–61.

Gasteiger E, Hoogland C, Gattiker A, Duvaud S, Wilkin M, Appel R, et al. Protein identification and analysis tools on the ExPasy server. In: Walker JM, editor. The proteomics protocols handbook. New Jersey: Humana Press; 2005. p. 571–607.

Gnutt D, Timr S, Ahlers J, König B, Manderfeld E, Heyden M, et al. Stability effect of quinary interactions reversed by single point mutations. J Am Chem Soc. 2019;141:4660–9.

Gronenborn AM, Filpula DR, Essig NZ, Achari A, Whitlow M, Wingfield PT, et al. A novel, highly stable fold of the immunoglobulin binding domain of streptococcal protein G. Science. 1991;253:657–61.

Guinn EJ, Schwinefus JJ, Cha HK, McDevitt JL, Merker WE, Ritzer R, et al. Quantifying functional group interactions that determine urea effects on nucleic acid helix formation. J Am Chem Soc. 2013;135:5828–38.

Guseman AJ, Perez Goncalves GM, Speer SL, Young GB, Pielak GJ. Protein shape modulates crowding effects. Proc Natl Acad Sci U S A. 2018;115:10965–70.

Guseman AJ, Pielak GJ. Cosolute and crowding effects on a side-by-side protein dimer. Biochemistry. 2017;56:971–6.

Guseman AJ, Speer SL, Perez Goncalves GM, Pielak GJ. Surface charge modulates protein-protein interactions in physiologically relevant environments. Biochemistry. 2018;57:1681–4.

Hermans J, Wang L. Inclusion of loss of translational and rotational freedom in theoretical estimates of free energies of binding. Application to a complex of benzene and mutant T4 lysozyme. J Am Chem Soc. 1997;119:2707–14.

Huggins ML. Thermodynamic properties of solutions of long-chain compounds. Ann N Y Acad Sci. 1942;43:1–32.

Jee J, Byeon I-JL, Louis JM, Gronenborn AM. The point mutation A34F causes dimerization of GB1. Proteins Struct Funct Bioinf. 2008;71:1420–31.

Knowles DB, Shkel IA, Phan NM, Sternke M, Lingeman E, Cheng X, et al. Chemical interactions of polyethylene glycols (PEGs) and glycerol with protein functional groups: applications to effects of PEG and glycerol on protein processes. Biochemistry. 2015;54:3528–42.

Kozer N, Schreiber G. Effect of crowding on protein–protein association rates: fundamental differences between low and high mass crowding agents. J Mol Biol. 2004;336:763–74.

Lekkerkerker HNW, Tuinier R. Colloids and the depletion interaction. Dordrecht: Springer; 2011.

Minton AP. Quantitative assessment of the relative contributions of steric repulsion and chemical interactions to macromolecular crowding. Biopolymers. 2013;99:239–44.

Nayar D. Molecular crowders can induce collapse in hydrophilic polymers via soft attractive interactions. J Phys Chem B. 2023;127:6265–76.

Niu S, Ruotolo BT. Collisional unfolding of multiprotein complexes reveals cooperative stabilization upon ligand binding. Protein Sci. 2015;24:1272–81.

Olgenblum GI. Crowding model implementation: A GitHub repository for the model code. Available at: https://github.com/giliolgenblum/crowdingmodel/ (Accessed February 22, 2025).

Olgenblum GI, Carmon N, Harries D. Not always sticky: specificity of protein stabilization by sugars is conferred by protein–water hydrogen bonds. J Am Chem Soc. 2023;145:23308–20.

Phillip Y, Sherman E, Haran G, Schreiber G. Common crowding agents have only a small effect on protein-protein interactions. Biophys J. 2009;97:875–85.

Sapir L, Harries D. Macromolecular stabilization by excluded cosolutes: mean field theory of crowded solutions. J Chem Theory Comput. 2015a;11:3478–90.

Sapir L, Harries D. Is the depletion force entropic? Molecular crowding beyond steric interactions. Curr Opin Colloid Interface Sci. 2015b;20:3–10.

Sarkar M, Li C, Pielak GJ. Soft interactions and crowding. Biophys Rev. 2013;5:187–94.

Schellman J. Protein stability in mixed solvents: a balance of contact interactions and excluded volume. Biophys J. 2003;85:108–25.

Smith CK, Withka JM, Regan L. A thermodynamic scale for the beta-sheet forming tendencies of the amino acids. Biochemistry. 1994;33:5510–7.

Sorichetti V, Hugouvieux V, Kob W. Determining the mesh size of polymer solutions via the pore size distribution. Macromolecules. 2020;53:2568–81.

Speer SL, Stewart C, Sapir L, Harries D, Pielak GJ. Macromolecular crowding is more than hard-core repulsions. Annu Rev Biophys. 2022;51:267–300.

Speer SL, Zheng W, Jiang X, Chu I-T, Guseman A, Liu M, et al. The intracellular environment affects protein-protein interactions. Proc Natl Acad Sci U S A. 2021;118:e2019918118.

Stadmiller SS, Pielak GJ. Protein-complex stability in cells and in vitro under crowded conditions. Curr Opin Struct Biol. 2021;66:183–92.

Stewart CJ, Olgenblum GI, Propst A, Harries D, Pielak GJ. Resolving the enthalpy of protein stabilization by macromolecular crowding. Protein Sci. 2023;32:e4573.

Sukenik S, Sapir L, Harries D. Balance of enthalpy and entropy in depletion forces. Curr Opin Colloid Interface Sci. 2013;18:495–501.

Theillet F-X, Binolfi A, Frembgen-Kesner T, Hingorani K, Sarkar M, Kyne C, et al. Physicochemical properties of cells and their effects on intrinsically disordered proteins (IDPs). Chem Rev. 2014;114:6661–714.

Timr S, Madern D, Sterpone F. Protein thermal stability. Prog Mol Biol Transl Sci. 2020;170:239–72.

Werle Y, Kovermann M. Fluorine labeling and ^{19}F NMR spectroscopy to study biological molecules and molecular complexes. Chem A Eur J. 2024; 31:e202402820.

Wyman J. Linked functions and reciprocal effects in hemoglobin: a second look. Adv Protein Chem. 1964;19:223–86.

Xie G, Timasheff SN. The thermodynamic mechanism of protein stabilization by trehalose. Biophys Chem. 1997;64:25–43.

Zhou H-X, Rivas G, Minton AP. Macromolecular crowding and confinement: biochemical, biophysical, and potential physiological consequences. Annu Rev Biophys. 2008;37:353–73.

Zhou Y-L, Liao J-M, Chen J, Liang Y. Macromolecular crowding enhances the binding of superoxide dismutase to xanthine oxidase: implications for protein–protein interactions in intracellular environments. Int J Biochem Cell Biol. 2006;38:1986–94.

Zosel F, Soranno A, Buholzer KJ, Nettels D, Schuler B. Depletion interactions modulate the binding between disordered proteins in crowded environments. Proc Natl Acad Sci U S A. 2020;117:13480–9.

SUPPORTING INFORMATION

Additional supporting information can be found online in the Supporting Information section at the end of this article.